PROCEEDINGS, TOUGH Symposium 2006
Lawrence Berkeley National Laboratory, Berkeley, California, May 15–17, 2006

THREE-DIMENSIONAL ANALYSES OF COUPLED GAS, HEAT AND NUCLIDE TRANSPORT IN A REPOSITORY INCLUDING ROCK SALT CONVERGENCE

Vijen Javeri

Gesellschaft für Anlagen- und Reaktorsicherheit (GRS) mbH
Schwertnergasse 1, 50667 Cologne, Germany
e-mail: vijen.javeri@grs.de

ABSTRACT

For a repository system for spent fuel elements in rock salt, coupled three-dimensional transport of gas, heat and nuclide is studied with a modified version of the computer code TOUGH2/EOS7R. Variable hydro-dynamic properties of compactable filling material like crushed salt are determined considering convergence of rock salt depending on fluid pressure and temperature. Among other observations, the analyses show that that a two-dimensional analysis can be sufficient and reasonable, if the gas transport in an isothermal configuration is a major issue. However, if the heat and/or nuclide transport are also to be investigated, a three-dimensional approach can be necessary to adequately quantify the consequences of the combined transport processes.

INTRODUCTION

To assess the long-term safety of a repository for heat-generating nuclear waste in a deep rock-salt formation, often a brine inflow into the repository is postulated. The brine can react with the radioactive waste or with its containers and can gradually disassemble them. The radioactive substances after being dissolved in brine can be transported out of the repository by rock convergence and subsequently can be released into the geosphere. The brine and nuclide transport out of the repository can also be enhanced by the decay heat sources and gas generation (mainly hydrogen) due to corrosion of metallic materials, at least in the vicinity of the disposal place.

In (Baudoin et al. 2000) the long-term radiological impacts of deep geological disposal of spent fuel in various host-rock formations (clay, crystalline rock and rock salt) are analyzed employing a one-dimensional network of a repository system but neglecting gas and heat transport. In (Javeri 2000), combined gas and nuclide transport including variable brine fraction and rock convergence is studied in an isothermal two-dimensional repository system in rock salt. To extend these previous analyses, coupled transport of gas, heat and nuclide in a simplified three-dimensional repository for spent fuel elements in rock salt is studied with the computer code TOUGH2/EOS7R, which is here enhanced to include:

- rock convergence depending upon porosity, pressure and temperature,
- variable porosity and permeability of compactable filling material such as crushed salt,
- two-phase fluid flow induced by variable rock convergence,
- heat conductivity and diffusion depending on temperature.

MODIFICATION OF TOUGH2 MODELS

With TOUGH2/EOS7R, two-phase flow, nuclide and heat transport with four liquid components (groundwater, brine, parent nuclide, daughter nuclide) and one gas component (air or hydrogen) in a three dimensional anisotropic porous configuration can be simulated (Pruess 1991; Oldenburg and Pruess 1995). The code uses an integral finite difference method with arbitrary volume elements of constant porosity and permeability to solve five mass conservation equations for five fluid components, and one energy equation for heat transport. To determine the reduction of porosity and permeability of a compactable filling material due to rock convergence, TOUGH2 is here extended to consider variable rock convergence depending upon pressure and temperature and also to consider the induced fluid and heat outflow due to porosity reduction in a volume element (Javeri 2000, Storck 1996):

$$n = n(p, T) = V_{Void}/V_{Element} \geq n_{min}, \qquad k = k(n),$$

$$n_t = (1/n)(dn/dt) = C_L/n,$$

$$C_L = C_{Ref}\, f_1(p)\, f_2(n)\, f_3(T), \quad C_L = 0, \text{ if } n \leq n_{min},$$

$$f_1 = (1 - p_{Fluid}/p_{Rock})^m \leq 1, \qquad f_1 = 0, \text{ if } p_{Fluid} \geq p_{Rock},$$

$$n_1 = 1 - n/n_{Ref}, \qquad n_2 = (nn_1)^{(1/m)},$$

$$f_2 = nn_1(n_1^2 + n_2)^{-m} \leq 1, \text{ if } n < n_{Ref},$$

$$f_2 = 1 \text{ if } n \geq n_{Ref},$$

$$\theta = T + 273.15, \qquad \theta_1 = (\theta - \theta_{Ref}) / (\theta_{Ref}\theta),$$

$$f_3 = [\exp(A_1\theta_1) + a \exp(A_2\theta_1)] / (1 + a) \geq 1.$$

The functions f_1, f_2 and f_3 describe the experimental observations regarding creeping behaviour of rock salt enveloping compactable back-fill material. The

resistance against rock convergence increases, if the pressure in the pores of the back fill increases and/or the porosity decreases. The creeping rate, or the convergence of the rock salt, increases rapidly if the temperature increases. The reduction of porosity of back fill leads to an additional fluid and enthalpy flow out of a volume element (i: liquid component):

$S_{Liquid} = V_{Liquid}/V_{Void}$, $\Sigma X_{Liquid,i} = 1$,

$Q_{Liquid,i,Por} = |nV_{Element}\, n_t\, \rho_{Liquid}\, S_{Liquid}\, X_{Liquid,i}|$,

$Q_{Gas,Por} = |nV_{Element}\, n_t\, \rho_{Gas}\, S_{Gas}|$, $S_{Gas} = V_{Gas}/V_{Void}$,

$H_{Liquid,Por} = Q_{Liquid,Por}\, h_{Liquid}$, $H_{Gas,Por} = Q_{Gas,Por}\, h_{Gas}$.

The original constant-heat conductivity of the solid component and molecular diffusion coefficient in the liquid phase in TOUGH2/EOS7R are replaced by appropriate functions of temperature (Javeri 2004):

$d(\theta) = d(\theta_{Ref})\, \exp[A_{Diff}(\theta - \theta_{Ref}) / (\theta\, \theta_{Ref})]$.

$\lambda_{Rock} = \lambda(T)$.

The agreement between the modified TOUGH2/ EOS7R and the analytical solution (Kinzelbach 1987) for nuclide transport including advection, anisotropic diffusion, decay and linear adsorption in a two dimensional infinite medium is satisfactory (Fig. A).

MODELING APPROACH

To analyze the combined influence of transient gas and heat generation and rock convergence on nuclide transport in a two-phase flow configuration, a three-dimensional model of a repository is considered (Javeri 2004). A horizontal disposal drift for the spent fuel elements with a transient decay heat production is located at a depth of 850 m in rock salt. The fuel elements are contained in a so-called Pollux cask (length: 5.46 m, diameter: 1.56 m) mainly made of fine grain steel MnNi 6.3. In a drift of 215 m horizontal length, 33 Pollux casks are emplaced maintaining a minimum axial distance of 1 m between the two neighboring casks. The drift is back-filled with compactable crushed salt. To avoid a temperature beyond 200 ^{o}C in rock salt, a minimum distance of 36 m between the parallel drifts is estimated. Accordingly, a width of 36 m in the y-direction in the present model is selected (Fig. 1).

The transient decay heat generation of a Pollux cask is given in Table 4. Assuming an interim storage period of 30 years for the required cooling before the emplacement of the spent fuel elements in the repository, the initial decay heat production amounts to 5.14 kW/cask at the beginning of the problem time t = 0. The total decay heat production of 33 casks is simulated by a transient homogeneous heat source in the material domain 4 located at the bottom of the drift. It is assumed that the repository is back-filled and sealed immediately after emplacement of the spent fuel elements. The region separating the main undisturbed rock salt from the drift is represented as an excavation-damaged zone with a higher permeability than the undisturbed rock salt. The drift is sealed with a relatively low-permeability material comparable to the excavation-damaged zone. The shaft is back-filled with a rather permeable material like gravel sand. It is postulated that from the very beginning the whole system except the drift is fully flooded and the drift is partly flooded with saturated salt water, which can react with the radioactive waste. The radioactive substances, after being dissolved in brine, can be transported out of the repository by rock convergence, decay heat and gas generation.

The dissolved radioactive substances in the drift are represented by a single nuclide with a half life of 10^4 years. The nuclide in the liquid phase is simulated by a transient nuclide source at the center of the drift with temporal variation as follows:

1. $0 \le t \le 1000$ years: linearly increasing nuclide source from 0 to 1 kg/year,
2. $1000 \le t \le 2000$ years: linearly decreasing nuclide source from 1 to 0 kg/year.

Further, brine pockets are postulated to exist in the repository system out of which, due to rock convergence, brine can enter into the drift. This inflow is simulated by a transient source at the right-hand end of the drift as follows:

1. $0 \le t \le 1000$ years: linearly increasing brine source from 0 to 100 kg/year,
2. $1000 \le t \le 2000$ years: linearly decreasing brine source from 100 to 0 kg/year.

Employing the estimation of gas generation due to corrosion in a repository for spent fuel elements in rock salt (Schulze 2002), a transient hydrogen source in the central part of the drift is introduced as follows:

1. $0 \le t \le 100$ years: linearly increasing hydrogen source from 0 to 3.84 kg/year,
2. $100 \le t \le 20000$ years: constant hydrogen source of 3.84 kg/year,
3. $20000 \le t \le 40000$ years: linearly decreasing hydro-gen source from 3.84 to 0 kg/year.

The fluid consists of three components: salt water, nuclide in liquid phase, and hydrogen. The solubility of hydrogen in the liquid phase is given by:

$X_{Gas\ in\ Liquid} = m_{Gas}/m_{Liquid} = (p/C_{Henry})(M_{Gas}/M_{Liquid})$.

To describe two-phase flow, the modified Brooks-Corey functions are used to calculate relative permeability and capillary pressure:

$S_{Liq,Eff} = (S_{Liquid} - S_{Liq,\,Res}) / (1 - S_{Liq,Res} - S_{Gas,Res})$,

$k_{Liq,Rel} = (S_{Liq,Eff})^4$, $k_{Liq} = kk_{Liq,Rel}$,

$k_{Gas,Rel} = (1 - S_{Liq,Eff})^2 (1 - S^2_{Liq,Eff})$, $k_{Gas} = kk_{Gas,Rel}$,

$p_{cap} = p_b(1 - S_{Liquid})/S_{Gas,Res}$, if $(1 - S_{Gas,Res}) \le S_{Liqid} \le 1$,

$p_{cap} = p_b / (S_{Liq,Eff})^{0.5}$, if $S_{Liquid} \le (1 - S_{Gas,Res})$,

$p_b = 0.56\ k^{-0.346}$, k in m², p_b in Pa.

Postulating constant molecular diffusion coefficient in the liquid phase and parameters listed in Tables 1 to 5 (Javeri 2004), four reference cases and three additional cases are defined:

Case	Heat source	Gas source	Rock convergence
NG1	No	Yes	No
NGK1	No	Yes	Yes
NWG1	Yes	Yes	No
NWGK1	Yes	Yes	Yes

Case	Reference convergence rate in 1/year	Permeability of sealing material and excavation damaged zone in m²
NWGK1	- 1E-3	1E-16
NWGK2	- 1E-3	1E-17
NWGK3	- 1E-3	1E-18
NWGK4	- 1E-4	1E-16

RESULTS

These cases are computed with the modified TOUGH2/EOS7R up to $t = 10^5$ years. Since strongly non-linear mass and heat conservation equations in a three-dimensional two-phase flow configuration with varying material properties are solved, the computational effort is relatively high. Some selected results regarding temperature, pressure, phase saturation, nuclide mass fraction, etc. are presented below. The vertical temperature profile at the center of the drift for the case NWG1 with constant hydrodynamic properties in Fig. 2 shows that the maximum temperature of 230 °C is reached at the center of the spent fuel element cask at t = 30 years and the maximum temperature of 175 °C at the interface between the filling material and the excavation-damaged zone remains below the admissible limiting temperature of 200 °C. The temperature distributions in the plane y = 18 m (central plane) and y = 4 m (boundary plane) indicate that the temperature varies noticeably in the y-direction (Fig. 3 and 4). At t = 1000 years the maximum temperature in the fuel elements is still around 92 °C and 84 °C in the boundary plane y = 4 m. Because of the decaying heat source, the maximum temperature of 49 °C in the fuel elements (y = 18 m) at $t = 10^4$ years is significantly lower than the corresponding value at t = 1000 years (Figs. 3 and 5).

The nuclide mass fraction in the liquid phase in Figs. 6 to 8 is to be compared with the maximum value of 0.02, which is reached at around t = 1300 years in the drift. Since the permeability of the rock salt (1E-20 m²) is very low and the brine enters at the right-hand end of the drift, within the first 2000 years, the nuclide migrates due to advection chiefly from right to left towards the shaft. After 2000 years, as the brine does not flow into the drift, the nuclide migrates more or less equally in all three directions by diffusion. Because of buoyancy effects, the gas saturation in the upper part of the drift and excavation-damaged zone is substantially higher than in the lower part (Fig. 9).

For an integral comparison, the temperature in the upper part of the crushed salt in the drift is depicted in Fig. 10. The maximum temperature of 168 °C occurs at t = 50 years in case NWGK3 with the lowest permeability (1E-18 m²) of sealing material and excavation-damaged zone. The temperature history is nearly the same in all cases, as the relatively low permeability does not allow noticeable convection and the heat conduction is less influenced by the rock convergence. The pressure in the upper part of the crushed salt in the drift indicates that without any heat source, the gas generation leads to a very limited pressure increment of less than 3 bar (Fig. 11). The rapid pressure build up from 99 up to 163 bar within the first 35 years in the cases with decay heat is caused by the increment of internal energy in a relatively closed system with a permeability k ≤ 1E-16 m² (Fig. 12). Such a high pressurization, very close to lithostatic pressure, can affect the mechanical stability of the filling or sealing material and repository substantially and can also lead to hydro-fracturing in the host rock. According to relatively low hydraulic diffusivity

$d_{hyd} = k / (n\mu\beta)$, $\beta = (1/\rho)(\partial\rho/\partial p)$,

the pressure decreases slowly, as the gas generation becomes effective. As expected, the maximum pressure increases, as the permeability of the sealing material and excavation-damaged zone decreases. The lower convergence rate in case NWGK4 leads to a slower porosity reduction in crushed salt and a little faster pressure reduction. Two more isothermal examples are also included in Fig. 12:

Case NGK3: same as case NWGK3, but no decay heat.

Case NGK32: same as case NGK3, but rock salt (material domain 1) is removed.

The pressure history of the three-dimensional case NGK3 can be reasonably well bracketed by the virtually two-dimensional case NGK32, as the rock salt with a very low permeability does not provide a noticeable transport capability for two-phase flow.

The porosity of the crushed salt in the upper part of the drift is depicted in Fig. 13. In case NWG1 without rock convergence, the porosity and the permeability of the crushed salt remain constant. In the isothermal case NGK1, the rock convergence is relatively low and, hence, the porosity reduction is slow leading to a final porosity of 0.045 at $t = 10^5$ years, still above the reference minimum value of 0.005. In the corresponding case NWGK1 with decay heat, significantly faster convergence rate and porosity reduction are observed [$f_3(T) \geq 1$] and the porosity reaches the minimum value of 0.005 at around t = 200 years. Subsequently, the rock convergence and the porosity change are stopped. With decreasing permeability of sealing material and excavation-damaged zone, the pressure in the drift increases in cases NWGK2 and NWGK3. This leads to a higher resistance against the rock convergence [$f_1(p) \leq 1$] and thereupon to a slower porosity reduction. As expected, in case NWGK4 with a lower convergence rate, the porosity reduction is slower and the final porosity of 0.053 is substantially higher than in case NWGK1.

The nuclide mass in the drift presented in Fig. 14 is to be compared with the maximum available mass of 1000 kg, which corresponds to the postulated nuclide source. Until around t = 1400 years, the nuclide mass increases and after that decreases as the decay with a half life of 1E4 years and the transport out of the drift become effective. Without heat source in the cases NG1 and NGK1, the nuclide removal is nearly the same, as the convergence rate and the driving force are limited. But in case NWGK1 with decay heat, the rock convergence and thereupon the nuclide removal is significantly faster than in case NWG1 without rock convergence. The nuclide outflow at the top boundary is less than 1E-10 kg/year compared to the maximum source of 1 kg/year. Fig. 15 shows the gas release at the top of the shaft. The gas outflow prior to the first minimum around t = 200 years can be explained by the gas removal due to thermal pressure increase in the initially partly flooded drift. Depending upon the parameters, the actual gas outflow starts between 150 and 300 years and reaches a steady state value of 3.84 kg/year, which corresponds to the postulated gas source in the drift. As at t = 2E4 years, the gas generation decreases, and the gas outflow also decreases. Fig. 15 indicates that practically all of the gas escapes from the shaft, as the rock salt has a very low permeability. Additional examples including d(θ) are reported in (Javeri 2004).

CONCUSIONS

In summary, from several two- and three-dimensional scoping analyses of combined gas, heat and nuclide transport under various conditions, one can conclude for the postulated repository system in rock salt:

(a) With decreasing permeability of sealing material and excavation of damaged zone, the pressure build-up due to gas generation in the drift increases.
(b) If the convergence of the rock salt is not considered, the decay heat production does not influence the nuclide removal and pressure build-up significantly, apart from the early pressurization due to rise in internal energy.
(c) If the convergence of rock salt is to be included, in an isothermal system, only a mild pressurization can be expected; but in the case of decay heat, a substantial pressurization in the drift and porosity reduction in crushed salt are to be expected.
(d) A two-dimensional analysis can be reasonable if gas transport in an isothermal configuration is a major issue. But if the heat and/or nuclide transport are to be studied, a three-dimensional approach is required to adequately quantify the consequences of the combined transport processes.

SYMBOLS

A: normalized activation energy [K]
c: specific heat [J/(kg C)]
d: molecular diffusion coefficient [m²/s]
H: enthalpy flow [J/s]
h: specific enthalpy [J/kg]
k: permeability [m²]
M: molecular weight [g/mol]
m: mass [kg]
m: stress parameter
n: porosity
p: pressure [Pa]
p_b : bubble entry pressure [Pa]
Q: mass flow [kg/s]
R: gas constant [J/(kg K)]
S: phase saturation
t: time [s]
T: temperature [°C]
V: volume [m³]
X: mass fraction
λ: heat conductivity [W/(m K)]
μ: dynamic viscosity [Pa s]
ρ: density [kg/m³]
θ: temperature [K]

REFERENCES

Baudoin, P. et al., *Spent fuel disposal performance assessment (SPA project): Final report,* Report EUR 19132EN, European Commission, Brussels, 2000.

Javeri, V., *Scoping analysis of combined gas and nuclide transport including variable brine fraction and rock convergence in a two dimensional repository,* Proc. Int. Conf. on Radioactive Waste Disposal (DisTec 2000), Germany, 465-470, 2000.

Javeri, V., *Dreidimensionale Analysen zum gekoppelten Gas-, Wärme- und Nuklidtransport in einem Endlager im Steinsalz,* Report GRS-A-3191, GRS, Germany, 2004 [limited distribution].

Kinzelbach, W., *Numerische Methoden zur Modellierung des Transports von Schadstoffen im Grundwasser,* Oldenbourg Verlag, Germany, 1987.

Oldenburg, C.M., and K. Pruess, *EOS7R: Radionuclide Transport for TOUGH2*, Lawrence Berkeley National Laboratory Report LBL-34868, Berkeley, USA, 1995.

Pruess, K., *TOUGH2-A general purpose numerical simulator for multiphase fluid and heat flow,* Lawrence Berkeley National Laboratory Report LBL-29400,, Berkeley, USA, 1991.

Schulze, O., *Auswirkungen der Gasentwicklung auf die Integrität gering durchlässiger Barrieregesteine,* Bundesanstalt für Geowissenschaften und Rohstoffe, Hannover, Germany, 2002 [limited distribution].

Storck, R. et al., *Das Programmpaket EMOS,* Report GRS-122, GRS, Germany, 1996.

Table 1. Discretization of three dimensional model

Horizontal x-axes (left to right)		Horizontal y-axes (left to right)		Vertical z-axes (top to bottom)	
N_x	Element length in m	N_y	Element length in m	N_z	Element length in m
1	8	1	8	6	20
4	24	1	5	2	10
5	43	1	3	1	8
4	24	1	1.3	1	5
		1	1.4	1	3
		1	1.3	1	1
		1	3	1	1.1
		1	5	1	1.4
		1	8	1	3
				1	5
				1	8
				2	10
				2	20
N: number of volume elements; N_{total} = 2646					

Table 2. Material properties

M	n	k m²	c J/(kgC)	λ W/(mC)	ρ kg/m³
1	0.001	1E-20	870	f(T)	2187
2	0.005	1E-16	870	f(T)	2187
3	0.2	k(n)	870	f(n) f(T)	1750
4	0.2	3.4E-12	477	15	7900
5	0.2	1E-16	900	2	2000
6	0.3	1E-12	900	2	2000
$k(n) = (4.752E\text{-}9\ m^2)\ n^{4.5}$				$f(n) = (1 - 2.91\ n)$	
$f(T) = 5.734 - 0.01838T + (2.86E\text{-}5)T^2 - (1.51E\text{-}8)T^3$, T in C					

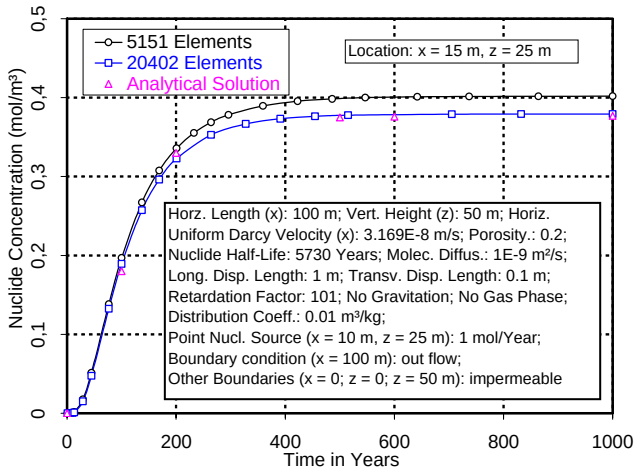

Figure A. Comparison of TOUGH2/EOS7R with the analytical solution for nuclide transport in an infinite (rectangular) homogeneous porous medium

Table 3. Location of material domains

M	Bottom left corner x	y	-z	Top right corner x	y	-z	N
2	8	16	156	319	20	153	27
2	0	16	162.5	319	20	159.5	30
3	104	16	158.1	319	20	156	30
3	104	16	159.5	319	17.3	158.1	5
3	104	18.7	159.5	319	20	158.1	5
4	104	17.3	159.5	319	18.7	158.1	5
5	80	16	159.5	104	20	156	9
6	8	16	159.5	80	20	156	27
6	0	16	159.5	8	20	0	42
1	2466 elements out side material domains 2 to 6						
M: Material domain; x, y, z in m							

Table 4. Decay heat production of a Pollux cask for PWR spent fuel elements (Burnup: 50 GWd/$t_{Heavy\ Metal}$;U-235-Enrichment: 4%).

Time since fuel element unloading in years	Decay heat production in kW/(Pollux cask)
0	8165
1	56.59
2	31.58
5	12.53
10	8.08
20	6.18
30 (t = 0 years)	5.14
50	3.71
100	2.02
200	1.12
500	0.62
1E3	0.35
1E4	0.08
1E5	0.01

Table 5. Hydrodynamic properties

Property	Value
Density of liquid phase	1.2 $\rho_{Water}(p,T)$
Dynamic viscosity of liquid phase	2 $\mu_{Water}(p,T)$
Dynamic viscosity of hydrogen	8.95 E-6 Pas
Gas constant of hydrogen	4124 J/(kgK)
Molecular weight of liquid phase	18 g/mol
Molecular weight of hydrogen	2 g/mol
Henry constant for hydrogen, C_{Henry}	1E11 Pa
Compaction of crushed salt	
Reference convergence rate, C_{Ref}	- 0.001 1/year
Stress parameter, m	4
Lithostatic pressure, p_{Rock}	160 bar
Minimum porosity, n_{min}	0.005
Reference porosity, n_{Ref}	0.3
Reference temperature, θ_{Ref}	313 K
Normalized activation energy, A_1	6500 K
Normalized activation energy, A_2	13000 K
Parameter in function $f_3(T)$, a	0.029
Two phase flow parameter	
Residual liquid saturation, $S_{Liq,Res}$	0.1
Residual gas saturation, $S_{Gas,Res}$	0.02
Diffusion parameter	
Mol. diffusion coefficient, $d_{Nuclide}$	1E-9 m²/s
Mol. diffusion coeff.,$d_{Dissolv.Hydrogen}$	1E-11 m²/s
Norm. activation energy, A_{Diff}	0 or 2525 K
Half life of nuclide	1E4 years

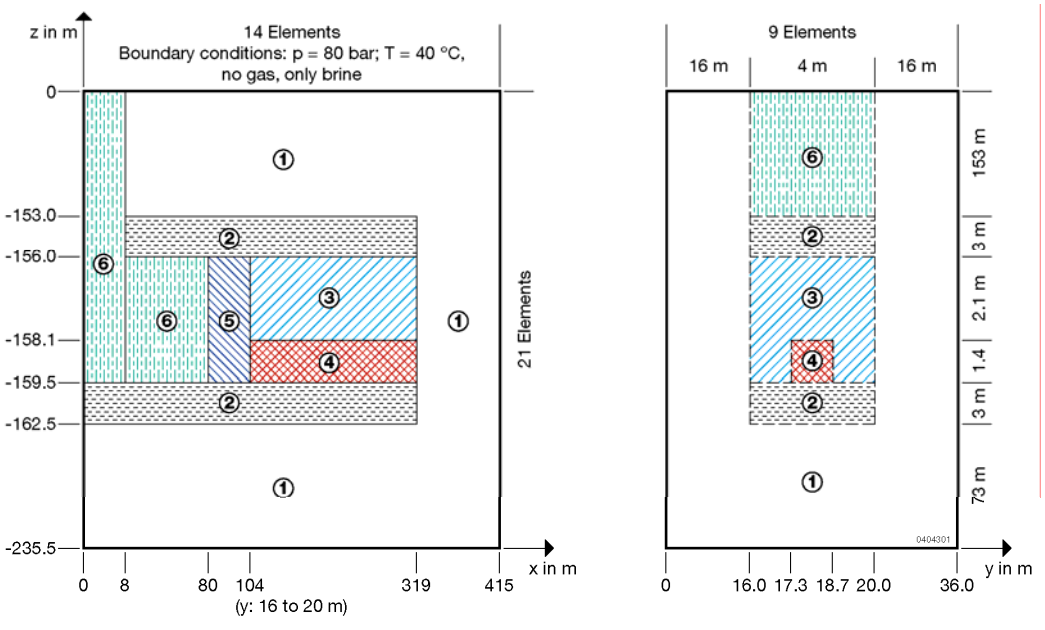

Figure 1. Three-dimensional model of a repository

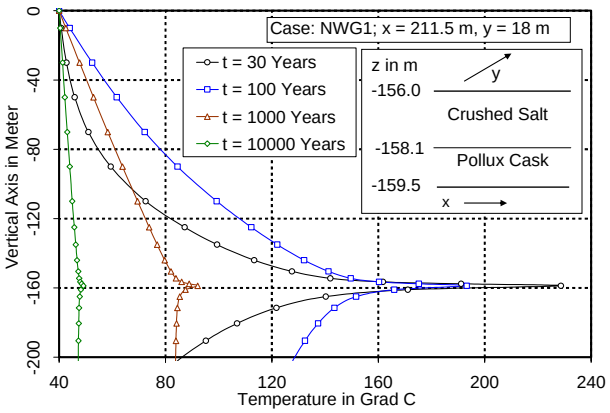

Figure 2. Vertical temperature profile in case NWG1

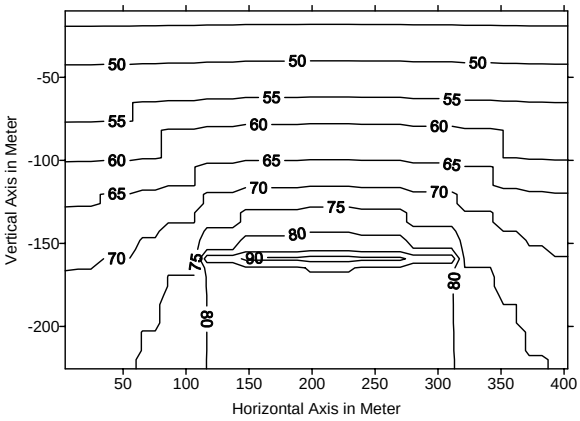

Figure 3. Temperature at y = 18 m and t = 1000 years in case NWG1

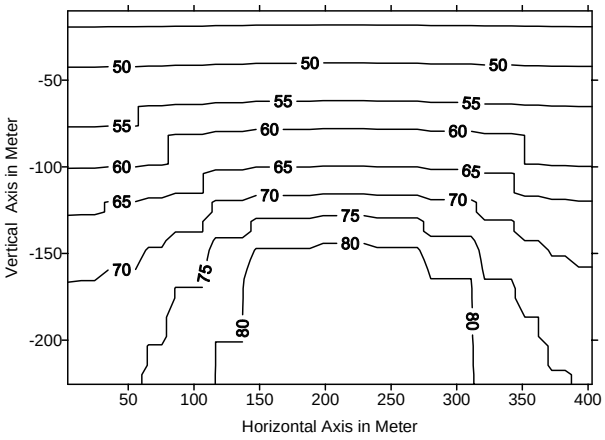

Figure 4. Temperature at y = 4 m and t = 1000 years in case NWG1

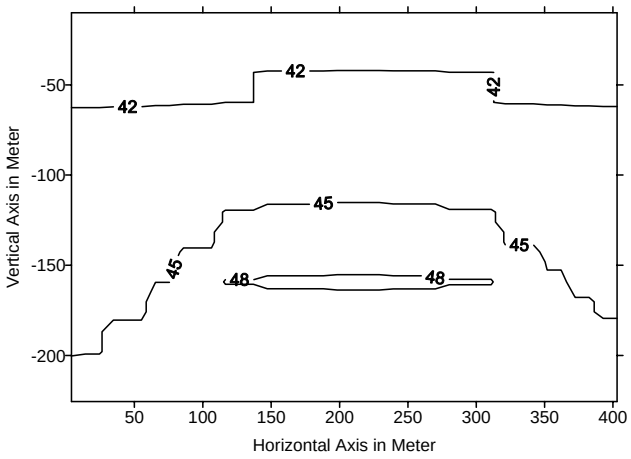

Figure 5. Temperature at y = 18 m and t = 10000 years in case NWG1

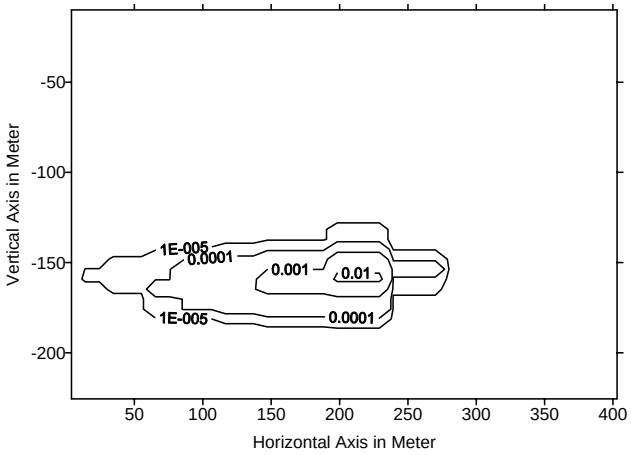

Figure 6. Nuclide mass fraction in liquid at y = 18 m and t = 1000 years in case NWG1

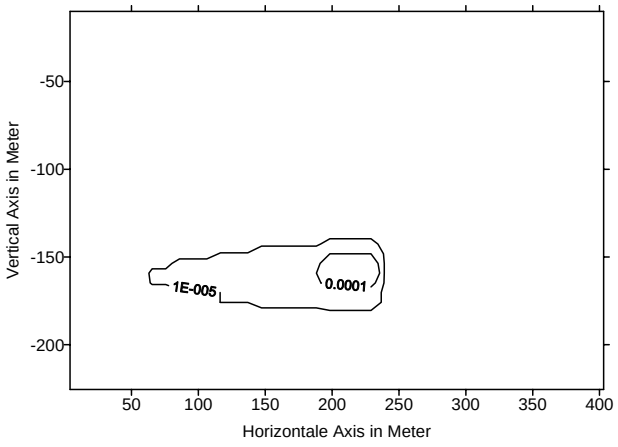

Figure 7. Nuclide mass fraction in liquid at y = 4 m and t = 1000 years in case NWG1

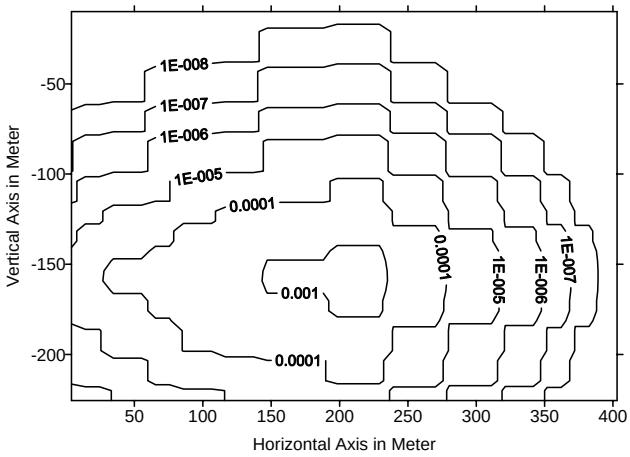

Figure 8. Nuclide mass fraction in liquid at y = 18 m and t = 10000 years in case NWG1

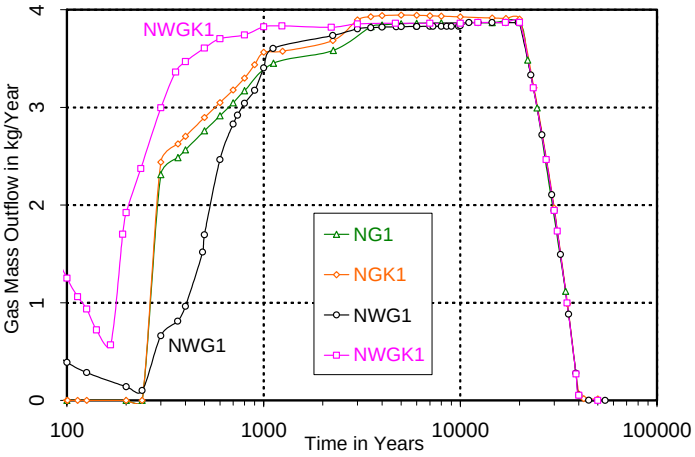

Figure 11. Pressure in the upper part of the crushed salt in drift (4 cases)

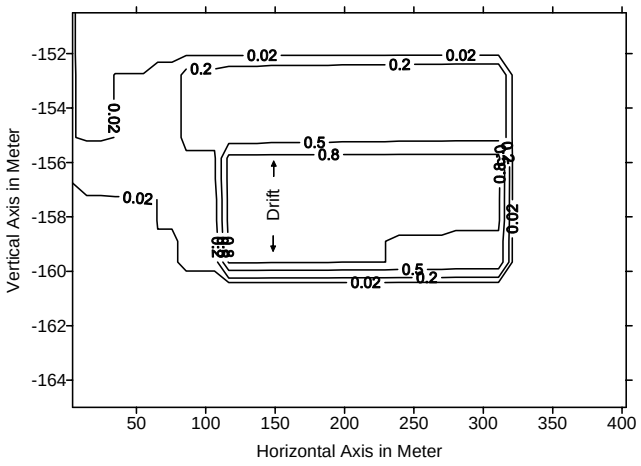

Figure 9. Gas saturation at y = 18 m and t = 1000 years in case NWG1

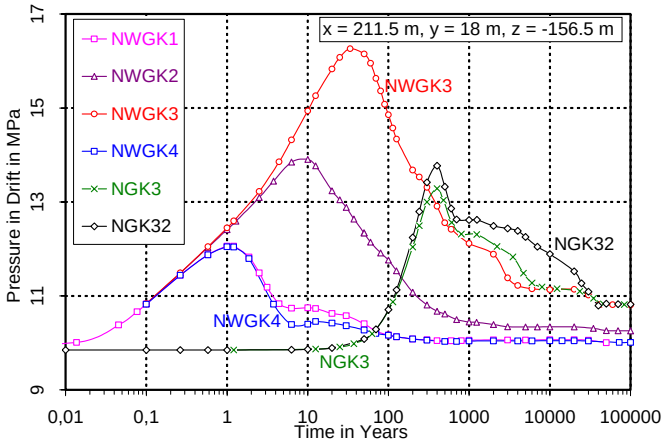

Figure 12. Pressure in the upper part of the crushed salt in drift (6 cases)

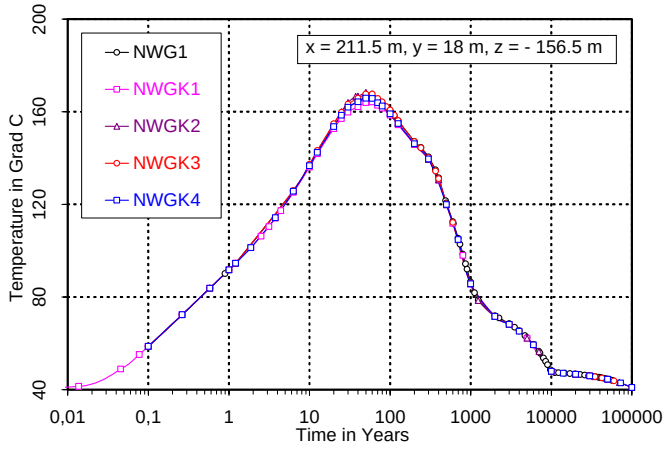

Figure 10. Temperature in the upper part of the crushed salt in drift

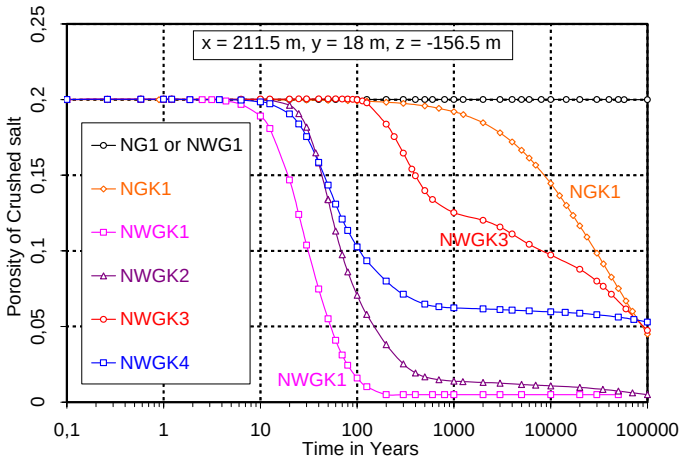

Figure 13. Porosity in the upper part of the crushed salt in drift

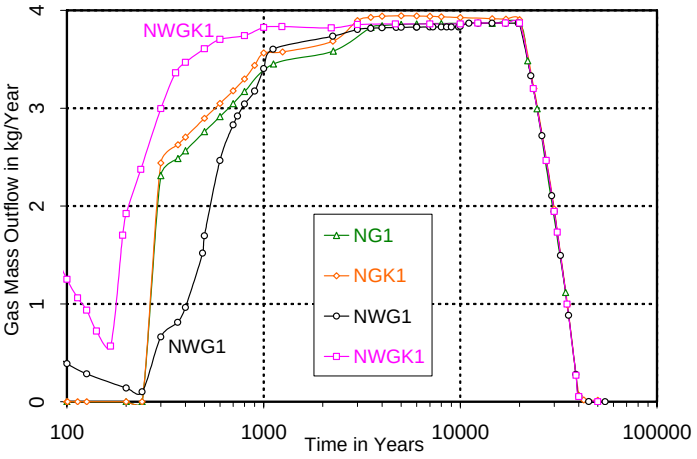

Figure 15. Gas mass outflow at the top of the shaft

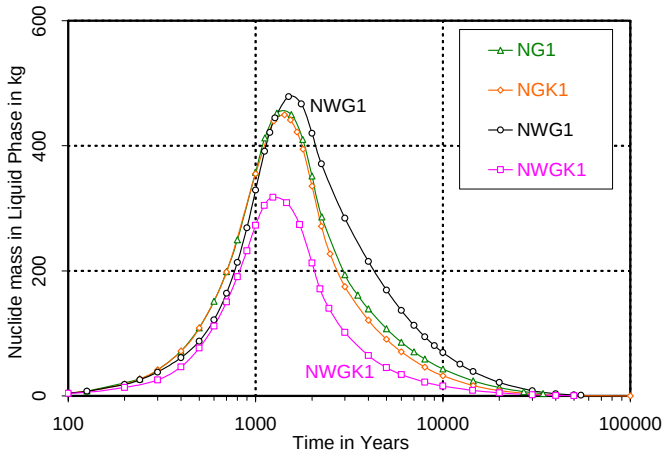

Figure 14. Nuclide mass in liquid phase in drift